Dissolution of alumina in cryolite melts: a conceptual DFT study

Alimet Sema ÖZEN*, **Zehra AKDENİZ**
Department of Maritime Transportation and Management Engineering,
Piri Reis University, İstanbul, Turkey

Abstract: Interactions between alumina and cryolite clusters were investigated using chemical reactivity descriptors based on conceptual DFT such as global hardness, η, global softness, S, fukui functions, f, and local softness, s. Hard and Soft Acids and Bases (HSAB) Principle was applied for identifying clusters that are most likely to interact with alumina, Al_2O_3. Local reactivity descriptors were employed to predict the most probable regions of interaction within the cluster.

Keywords: Cryolite-Al_2O_3, charged clusters, DFT, Fukui functions

1. Introduction

Metallic aluminum is produced at the industrial scale by the Hall-Heroult process [1, 2]. This process involves reduction of molten alumina (Al_2O_3) by electrolysis. Since Al_2O_3 has a very high melting point, around 2072 °C, molten cryolite (Na_3AlF_6) is added to form a eutectic solution and lower the melting temperature below 1000 °C. Apart from dissolving alumina, molten cryolite also acts as an electrolyte to increase conductivity during the electrolysis process [3]. Reduction of alumina takes place at the Al cathode and oxygen combines with carbon anode to form CO_2:

$$2Al_2O_3 \text{ solution } + C(s) \rightarrow Al(l) + CO_2(g). \tag{1.1}$$
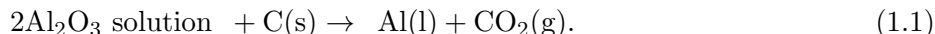
In order to optimize the process parameters, it becomes important to understand the role played by molten cryolite. There are many studies within the literature focusing on different electrolytes or combinations of different cations with AlF_3 [4–13]. Present study aims to understand interactions between alumina and molten cryolite at the molecular level using chemical reactivity indices within the conceptual Density Functional Theory (DFT) [14–16]. It is a further step after our previous work [17] by introducing interactions with Al_2O_3 and reactivity descriptors for predicting their extend.

Conceptual DFT focuses on matching chemical concepts such as electronegativity, electronic chemical potential, hardness or softness with the response of the electron density to perturbations introduced into the charge distribution. It uses principles such as Sanderson's electronegativity equalization principle, and Pearson's hard and soft acids and bases principle and maximum hardness principle for predicting chemical reactivity trends and reaction mechanisms [18, 19]. In this study, chemical reactivity indices based on conceptual DFT, such as global hardness, fukui functions and

---

*Correspondence: asozen@pirireis.edu.tr

local softness, are used to achieve a better understanding of the effect of local cryolite structure on the interactions with alumina. This approach was successfully applied before to understand the reactivity trends of Group 2B metal halides [20].

Within the conceptual DFT, hardness, η, is a global property describing the resistance to changes in electronic charge [15]. It can be described as how electronic chemical potential, μ, changes by changing the number of electrons, N, under constant external potential due to nuclei, $v(r)$. In the finite difference approximation this is equivalent to the difference between vertical ionization energy and electron affinity. For closed shell molecules it can be further approximated as the HOMO-LUMO energy gap:

$$\eta = \left(\frac{\partial \mu}{\partial N} \right)_{v(r)}$$

$$\eta = E_{\text{HOMO}} - E_{\text{LUMO}}.$$

(1.2)

Global softness, S, is the inverse of global hardness:

$$S = \frac{1}{\eta}.$$

(1.3)

The local softness, $s(r)$, describes the local response of the electron density $\rho(r)$ upon a change in the electronic chemical potential[4−6]:

$$s(\vec{r}) = \left(\frac{\partial \rho(\vec{r})}{\partial \mu} \right)_{v(r)}.$$

(1.4)

Local softness is related to global softness via the Fukui function, $f(r)$. It measures the response of the system to an external perturbation at a particular point. Fukui function is a chemical reactivity descriptor giving information about the local change in the electron density of an atom or molecule upon changing the total number of electrons:

$$f(\vec{r}) = \left(\frac{\partial \mu}{\partial v(\vec{r})} \right)_N = \left(\frac{\partial \rho(\vec{r})}{\partial N} \right)_{v(\vec{r})}.$$

(1.5)

The two local properties $s(r)$ and $f(r)$ are related to each other through the global softness, S,

$$s(\vec{r}) = f(\vec{r}) \, S$$

(1.6)

$f^+(r)$ is the reactivity index for a nucleophilic attack, $f^-(r)$ for an electrophilic attack and $f^0(r)$ for a radical attack. Within the finite difference approximation, these relationships can be written as:

$$f^+(\vec{r}) = \rho_{N+1}(\vec{r}) - \rho(\vec{r})$$
$$f^-(\vec{r}) = \rho_N(\vec{r}) - \rho_{N-1}(\vec{r})$$
$$f^0(\vec{r}) = \frac{1}{2} \left[\rho_{N+1}(\vec{r}) - \rho(\vec{r}) \right].$$

(1.7)

A condensed form of these functions employs the atomic populations q_k:

$$f^+ = q_k(N+1) - q_k(N)$$
$$f^- = q_k(N) - q_k(N-1) \qquad (1.8)$$
$$f^0 = \frac{1}{2}\big[q_k(N+1) - q_k(N-1)\big].$$

Global reactivity indices are very helpful in predicting whether there will be an interaction between two entities before they meet and, if the interaction is very likely, local reactivity indices will be pointing out the most probable regions of interaction within the molecules. All this information is very important in resolving the mechanism of a reaction.

2. Methodology

Cluster geometries obtained by the ionic model [4] are used as initial geometries in DFT calculations. For a detailed information about this methodology please refer to our recent work [17]. All of the structures are optimized at the M06-2X/6-31+G(d,p) level of theory. Gaussian 09 programme was used for geometry optimizations [21]. All stationary points have been characterized by normal mode analysis at the corresponding level of theory. Charge analysis has been carried out by using full natural population analysis (NPA).

3. Results and discussion
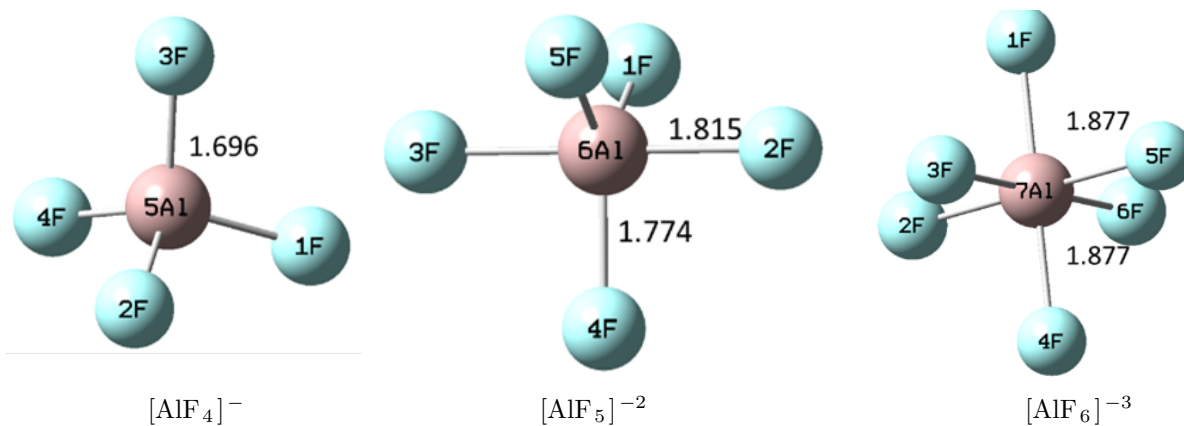
3.1. Global reactivity indices

In this study, most probable local structures present in the cryolite melt, such as AlF_4^-, AlF_5^{-2}, AlF_6^{-3}, their sodium salts forming Na_3AlF_6 as well as their dimers, are taken into account. Figure 1 shows optimized geometries for cryolite structures and Al_2O_3 at the M06-2X/-311+G(d) level.

The structures of cryolite clusters shown in Figure 1 are consistent with the previous computational studies [6, 8, 12]. The Al_2O_3 geometries were selected among the structures found by Li et al. [6]. On the other hand, they found the kite shape structure of Al_2O_3 to be more stable by 0.1 eV. The reason for this difference between two studies might lie in the methodologies applied. Genetic algorithm (GA) with density functional theory method was employed in their study with optimizations at the B3LYP/3-21G level, which a lower level of theory than the present one.
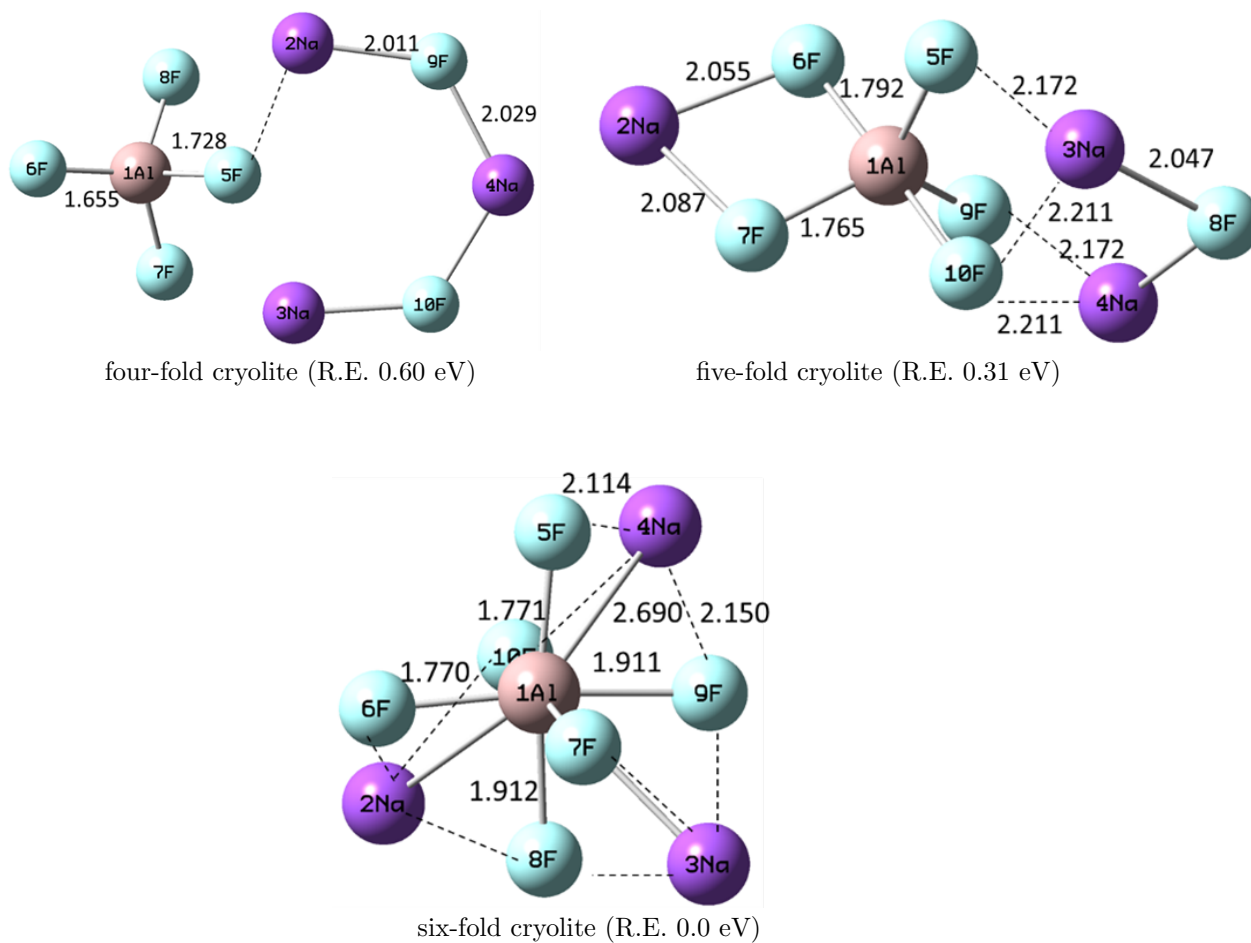
Table 1 shows the frontier orbital energies (highest occupied molecular orbital, HOMO and lowest unoccupied molecular orbital, LUMO) and global hardness, η, and global softness, S, values. $\Delta\eta$ value represents the global hardness difference between the cryolitic species and Al_2O_3.

According to hard and soft acids and bases theory, hard acids prefer to react with hard bases and soft acids prefer to react with soft bases [19]. Data presented in Table 1 shows that most likely interaction will take place between Al_2O_3 and AlF_6^{-3} for having very small difference in hardness ($\Delta\eta = 0.0105$). Hardness of five-fold Na_3AlF_6 is also close to Al_2O_3. These two are followed by AlF_5^{-2} and six-fold Na_3AlF_6. Cryolite is known to have a six-fold structure in the solid state. In the molten state, there is a mixture of four-, five- and six-fold structures depending on the cryolite ratio, CR (NaF/AlF$_3$) [22, 23]. So, Al_2O_3 and cryolite might start to interact through six-fold and

---

(a) $[\mathbf{AlF}_n]^{n-3}$ ions [17]

$[\mathrm{AlF}_4]^-$ $[\mathrm{AlF}_5]^{-2}$ $[\mathrm{AlF}_6]^{-3}$

(b) Cryolite ($\mathbf{Na_3AlF_6}$) clusters [17]

four-fold cryolite (R.E. 0.60 eV)   five-fold cryolite (R.E. 0.31 eV)

six-fold cryolite (R.E. 0.0 eV)

(c) Na_4AlF_{10} clusters [17]

$AlF_4^- - AlF_4^-$ cluster (R.E.=1.43 eV)

$AlF_4^- - AlF_5^{-2}$ cluster (R.E.=0.0 eV)

$AlF_5^{-2} - AlF_5^{-2}$ cluster (R.E. =0.56 eV)

(d) Al_2O_3 geometries

R.E. =0.63 eV

R.E. = 0.0 eV
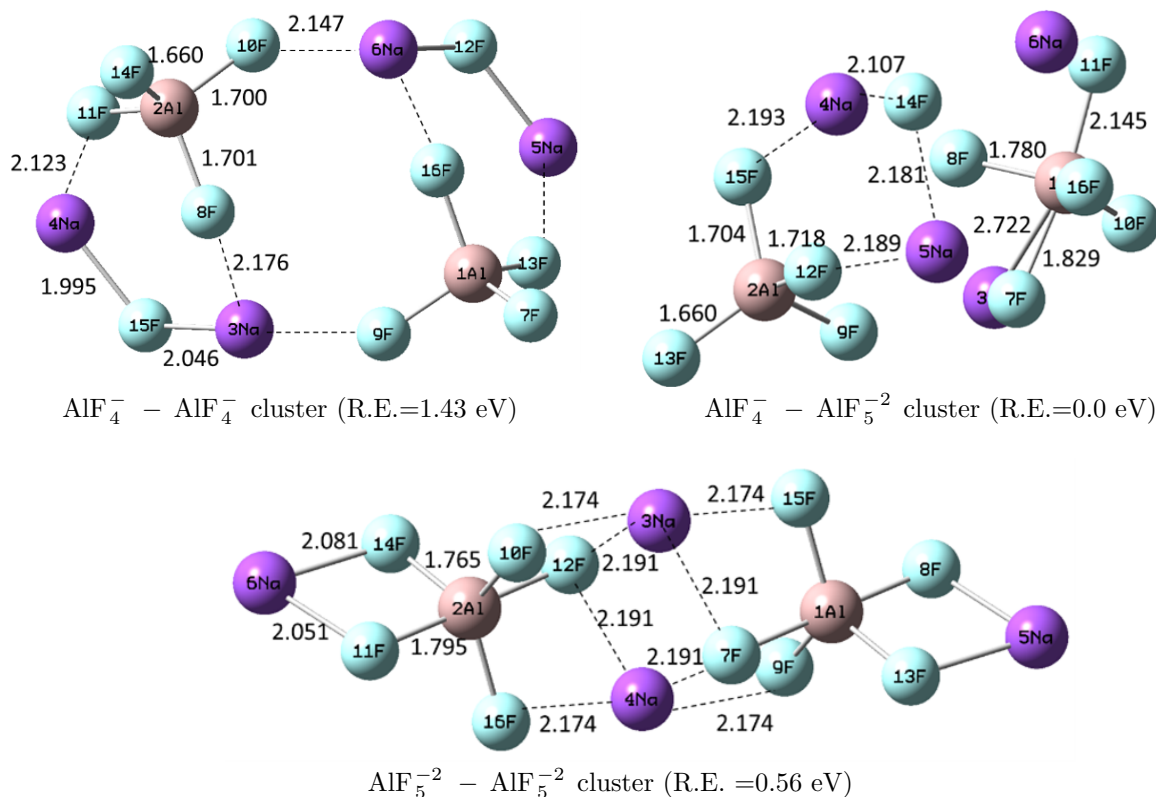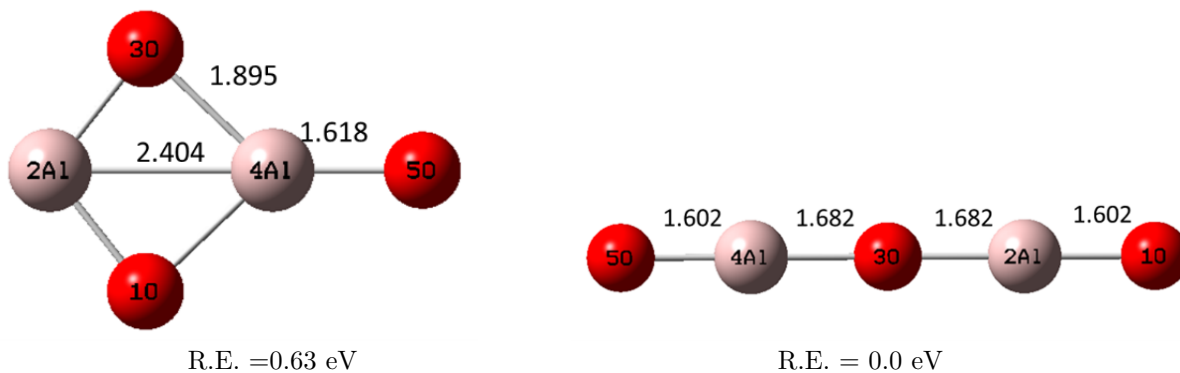
Figure 1. Optimized structures at the M06-2X/6-31+G(d,p) level **(a)** $[AlF_n]^{n-3}$ ions with four-, five-, and six-fold coordinationed geometries, namely $[AlF_4]^-$, $[AlF_5]^{-2}$ and $[AlF_6]^{-3}$, respectively. **(b)** Cryolite (Na_3AlF_6) clusters with four-, five-, and six-fold coordinations. **(c)** Na_4AlF_{10} clusters with two four-fold coordination $(AlF_4^- - AlF_4^-)$, one four-fold and one five-fold $(AlF_4^- - AlF_5^{-2})$, and two five-fold $(AlF_5^{-2} - AlF_5^{-2})$ coordinated structures. **(d)** Al_2O_3 geometries. Bond lengths in Å, relative energies (R.E.) in eV. Most stable conformer is shown in bold.

Table 1. Highest occupied molecular orbital and HOMO, lowest unoccupied molecular orbital, LUMO energies, global hardness, η, global softness, S, values and global hardness difference between the cryolitic species and Al_2O_3, $\Delta\eta$ at the M06-2X/6-31+G(d,p) level (All units in Hartrees).

Structure	HOMO	LUMO	η	S	$\Delta\eta$
Al_2O_3	-0.356	-0.111	0.245	4.080	
AlF_4^-	-0.275	0.140	0.415	2.408	0.1701
AlF_5^{-2}	-0.037	0.271	0.308	3.24	0.0630
AlF_6^{-3}	0.144	0.378	0.235	4.263	0.0105
F^-	-0.064	0.454	0.517	1.933	0.272
Na^+	-1.589	-0.241	1.348	0.742	1.103
Na salts					
Na_3AlF_6 (four-fold)	-0.384	-0.028	0.356	2.806	0.1113
Na_3AlF_6 (five-fold)	-0.348	-0.053	0.295	3.394	0.0496
Na_3AlF_6 (six-fold)	-0.376	-0.031	0.345	2.901	0.0996
$AlF_4^- - AlF_4^-$	-0.388	-0.038	0.350	2.860	0.1045
$AlF_4^- - AlF_5^{-2}$	-0.4181	-0.038	0.380	2.633	0.1347
$AlF_5^{-2} - AlF_5^{-2}$	-0.403	-0.047	0.356	2.812	0.1105
Na_2F	-0.544	-0.173	0.372	2.692	0.1264

five-fold local structures present in the melt first and these structures might have a prominent effect in the initiation of the dissolution process.

Figure 2 visualizes HOMO-LUMO energy data given in Table 1. Five-and six-fold cryolite have the closest HOMO energies to Al2O3. When LUMO levels are compared, structures with five-fold motifs still remain closer to Al_2O_3 (molecules are sorted according to the LUMO levels in Figure 2). Although hardness values, as represented by the difference in HOMO-LUMO energies, of AlF_6^- and Al_2O_3 are very close, the numerical values of the energies are quite far. That might be pointing out the role of the cations in these systems.

3.2. Local reactivity indices

Local reactivity indices such as fukui functions for nucleophilic and electrophilic attck, $f+$ and $f-$, respectively and related local softness values are tabulated in Table 2. Local softness differences, Δs, that are used for softness matching analyses are calculated between Al atom in Al_2O_3 and Al and F atoms from the cryolitic structures. Fukui functions provide information about the intramolecular reactivity while local softness values are related to the intermolecular reactivity. When two molecules are met, local softness matching between the atoms on both sides indicates the most likely regions of interaction.

After a comprehensive analysis of Table 2, the most likely regions of interaction with the Al atoms of Al_2O_3 are found to be F9 and F10 atoms in four-fold cryolite (CR = 2), F12 and F15 atoms in $Na_4Al_2F_{10}$ cluster (CR = 3) with two four-fold structure, and F14 in $Na_4Al_2F_{10}$ cluster
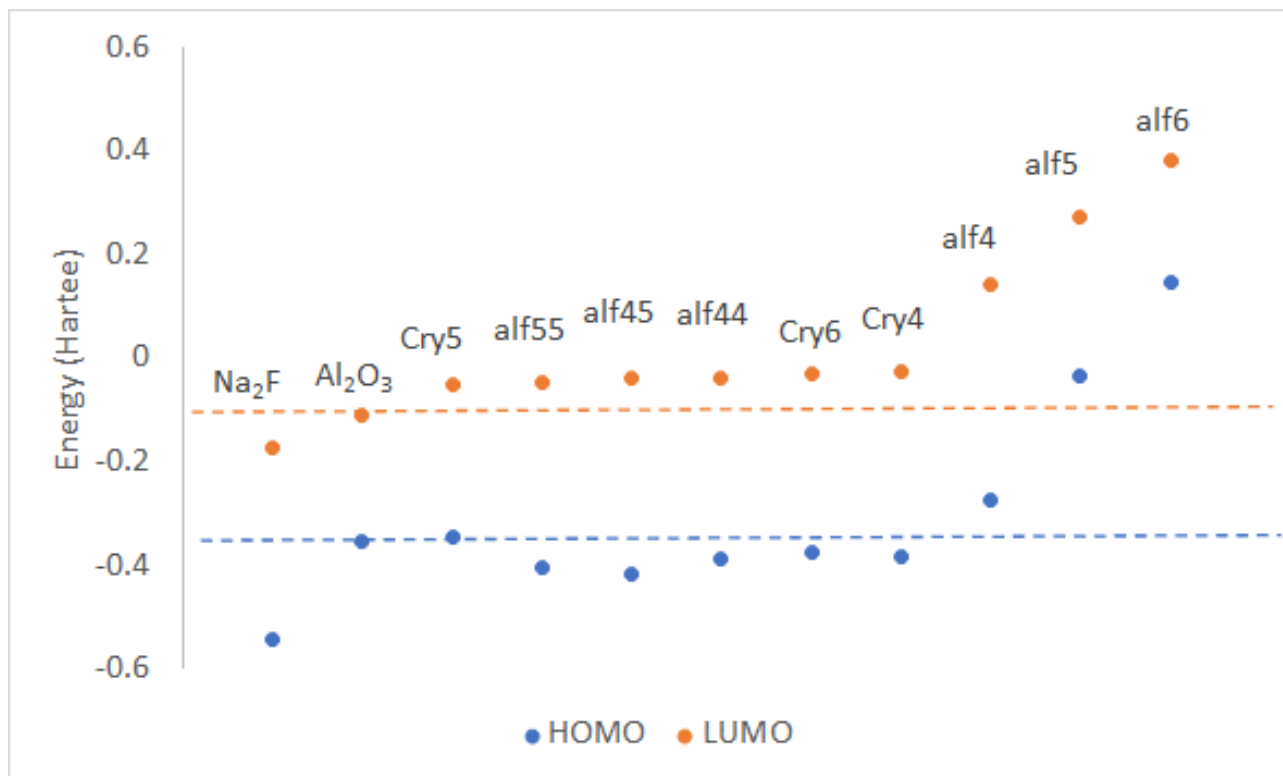
Figure 2. HOMO and LUMO levels of the molecules discussed. Molecules are sorted according to the LUMO levels (energies in Hartrees, Cryx=x-fold cryolite, alfxy=AlF$_x^-$ AlF$_y^-$).

with four-fold and five-fold structures (please see Figure 1 for atomic numbering). These fluorine atoms are either in the free ionic form within the cluster or in connection with two sodium atoms forming Na$_2$F$^+$ ion. On the other hand, local softness matching is not observed between the fluorines in isolated Na$_2$F$^+$ or F$^-$ ions and Al in Al$_2$O$_3$, for giving a larger Δs values. Therefore, four-fold motif is considered to be important for increasing solubility of Al$_2$O$_3$ by strengthening the interaction with fluorine atoms.

Δs values were also calculated between Al in Al$_2$O$_3$ and Na atoms. The main motivation here was the idea that atoms with similar softness values, in other words with similar susceptibility to nucleophilic attack, might undergo similar types of reactions. It was expected to obtain some sort of secondary reactivity information by comparing s^+ values. As seen in Table 2, Na5 and Na6 atoms in Na$_4$Al$_2$F$_{10}$ cluster (CR = 3) with two five-fold structures and Na atoms in Na$_2$F$^+$ have s^+ values very close to Al in Al$_2$O$_3$.

Combining these two reactivity indicators, it is possible to conclude that increasing CR ration increases the change for dissolution of Al$_2$O$_3$ in cryolite melts. Also, four-fold and five-fold motifs have some role in enhancing the interactions between fluorine ions and Al in Al$_2$O$_3$, increasing the solubility.

Table 2. Local reactivity indices: Fukui function for nucleophilic attack, $f+$, Fukui function for electrophilic attack, $f-$, local softness for nucleophilic attack, $s+$, and local softness for electrophilic attack, $s-$. Δs values represent the difference between $s+$ values of Al_2O_3 and $s-$ and $s+$ values of F and Al atoms in the other entities, respectively.

		$f+$	$f-$	$s+$	$s-$	Δs
Al_2O_3	O1	0.1220	0.3923	0.4978	1.6005	
	Al2	0.3397	0.1102	1.3859	0.4495	
	O3	0.0768	-0.0019	0.3133	-0.0078	
	Al4	0.3395	0.1094	1.3853	0.4464	
	O5	0.1220	0.3900	0.4976	1.5914	
AlF_4^-	F1	0.0169	0.2534	0.0407	0.6102	0.7757
	F2	0.0168	0.2553	0.0404	0.6145	0.7714
	F3	0.0169	0.2539	0.0407	0.6115	0.7744
	F4	0.0170	0.2541	0.0409	0.6119	0.774
	Al5	0.9324	-0.0167	2.2456	-0.0401	0.8597
AlF_5^{-2}	F1	0.0224	0.1836	0.0725	0.5959	0.79
	F2	0.0181	0.3182	0.0588	1.0330	0.3529
	F3	0.0181	0.3182	0.0589	1.0328	0.3531
	F4	0.0230	0.0289	0.0748	0.0937	1.2922
	F5	0.0223	0.1805	0.0723	0.5858	0.8001
	Al6	0.8961	-0.0294	2.9086	-0.0953	1.5227
AlF_6^{-3}	F1	0.0273	0.2486	0.1164	1.0596	0.3263
	F2	0.0273	0.0220	0.1165	0.0938	1.2921
	F3	0.0273	0.2484	0.1164	1.0589	0.327
	F4	0.0273	0.2486	0.1164	1.0596	0.3263
	F5	0.0273	0.022	0.1165	0.0938	1.2921
	F6	0.0273	0.2484	0.1164	1.0589	0.327
	Al7	0.8361	-0.0380	3.5639	-0.1620	2.178
Na_3AlF_6 (fourfold)	Al1	0.0078	0.0016	0.0219	0.0044	1.364
	Na2	0.2644	0.0046	0.7417	0.0130	0.6442
	Na3	0.2644	0.0046	0.7417	0.0130	0.6442

		$f+$	$f-$	$s+$	$s-$	Δs
$Na_4Al_2F_{10}$ − AlF_4^- − AlF_4^-	Al1	-0.0005	-0.0011	-0.0013	-0.0027	
	Al2	-0.0005	-0.0011	-0.0012	-0.0028	
	Na3	0.0281	0.0032	0.0714	0.0081	1.3145
	Na4	0.4593	0.0052	1.1685	0.0131	0.2174
	Na5	0.4502	0.0052	1.1455	0.0132	0.2404
	Na6	0.0286	0.0032	0.0727	0.0080	1.3132
	F7	0.0043	0.0109	0.0109	0.0278	1.3581
	F8	0.0021	-0.0043	0.0054	-0.0109	1.3968
	F9	0.0019	-0.0028	0.0048	-0.0071	1.393
	F10	0.0020	-0.0027	0.0051	-0.0068	1.3927
	F11	0.0005	-0.0002	0.0013	-0.0005	1.3864
	F12	0.0086	0.4889	0.0219	1.2440	0.1419
	F13	0.0007	-0.0001	0.0018	-0.0003	1.3862
	F14	0.0043	0.0109	0.0109	0.0278	1.3581
	F15	0.0084	0.4892	0.0214	1.2446	0.1413
	F16	0.0021	-0.0043	0.0053	-0.0110	1.3969
$Na_4Al_2F_{10}$ − AlF_4^- − AlF_5^{-2}	Al1	0.0175	-0.0248	0.0460	-0.0653	1.3399
	Al2	-0.0012	-0.0038	-0.0030	-0.0099	
	Na3	0.0103	0.0058	0.0270	0.0152	1.3707
	Na4	0.08849	0.0033	0.2330	0.0082	1.1529
	Na5	0.1317	0.0042	0.3467	0.0110	1.0392
	Na6	0.6961	0.0066	1.8325	0.0174	0.4466
	F7	0.0067	0.1976	0.0177	0.5201	0.8658
	F8	0.0049	0.1402	0.0128	0.3690	1.0169
	F9	0.0015	0.0035	0.0039	0.0092	1.3767
	F10	0.0055	0.0468	0.0146	0.1232	1.2627

Table 2. *continued.*

Na3AlF6 (fourfold)	Na4	0.4127	0.0041	1.1578	0.0115	0.2281	$Na_4Al_2F_{10}$ – AlF_4^- AlF_5^{-2}	F11	0.0040	0.0816	0.0106	0.2147	1.1712
	F5	0.0037	-0.009	0.0103	-0.0269	1.4128		F12	0.0013	-0.0050	0.0035	-0.0130	1.3989
	F6	0.0037	0.0123	0.0104	0.0345	1.3514		F13	0.0034	0.0139	0.0090	0.0365	1.3494
	F7	0.0047	0.0004	0.0132	0.0013	1.3846		F14	0.0215	0.4578	0.0567	1.2051	0.1808
	F8	0.0047	0.0004	0.0132	0.0013	1.3846		F15	0.0036	0.0037	0.0093	0.0097	1.3762
	F9	0.017	0.4908	0.0477	1.3769	0.009		F16	0.0046	0.0689	0.01224	0.1815	1.2044
	F10	0.017	0.4908	0.0477	1.3769	0.009		Al1	0.0004	-0.0107	0.0013	-0.0301	1.3846
Na3AlF6 (fivefold)	Al1	0.0058	-0.0058	0.0198	-0.0196	1.3661		Al2	0.0004	-0.0107	0.0013	-0.0301	1.3846
	Na2	0.9805	0.0043	3.3274	0.0146	1.9415	$Na_4Al_2F_{10}$ – AlF_5^{-2} AlF_5^-	Na3	0.0042	0.0066	0.0119	0.01867	1.374
	Na3	0.0067	0.0044	0.0227	0.0150	1.3632		Na4	0.0042	0.0066	0.0119	0.01867	1.374
	Na4	0.0067	0.0044	0.0227	0.0150	1.3632		Na5	0.4970	0.0067	1.3974	0.01892	0.0115
	F5	0.0028	0.0037	0.0094	0.0126	1.3733		Na6	0.4969	0.0067	1.3974	0.01892	0.0115
	F6	-0.0042	0.0087	-0.0143	0.0294	1.3565		F7	0.0007	0.1108	0.0019	0.3116	1.0743
	F7	-0.0058	0.0142	-0.0195	0.0481	1.3378		F8	-0.0021	0.1479	-0.0059	0.4160	0.9699
	F8	0.0018	0.9431	0.0062	3.2004	1.8145		F9	0.0012	0.1113	0.0034	0.3129	1.073
	F9	0.0028	0.0037	0.0094	0.0126	1.3733		F10	0.0012	0.1113	0.0034	0.3129	1.073
	F10	0.0029	0.0193	0.0099	0.0655	1.3204		F11	-0.0021	0.1480	-0.0059	0.4160	0.9699
Na3AlF6 (sixfold)	Al1	0.0161	-0.0350	0.0467	-0.1014	1.3392		F12	0.0007	0.1108	0.0019	0.3116	1.0743
	Na2	0.3097	0.0121	0.8984	0.0352	0.4875		F13	-0.0026	0.0160	-0.0074	0.0450	1.3409
	Na3	0.3094	0.0121	0.8975	0.0352	0.4884		F14	-0.0026	0.0160	-0.0074	0.0450	1.3409
	Na4	0.3116	0.011	0.9040	0.0335	0.4819		F15	0.0012	0.1113	0.0034	0.3129	1.073
	F5	0.0091	0.2155	0.0264	0.6253	0.7606		F16	0.0012	0.1113	0.0034	0.3129	1.073
	F6	0.0091	0.198	0.0264	0.5744	0.8115	Na_2F^+	F	-0.0108	0.9925	-0.0291	2.6714	1.2855
	F7	0.0091	0.1957	0.0264	0.5677	0.8182		Na	0.5054	0.0038	1.3604	0.0101	0.0255
	F8	0.0086	0.2225	0.0250	0.6455	0.7404		Na	0.5054	0.0038	1.3604	0.0101	0.0255
	F9	0.0087	0.0824	0.0251	0.2392	1.1467	F^-	F	1	1	1.933	1.933	0.5471
	F10	0.0086	0.0850	0.0251	0.2465	1.1394	Na^+	Na	1	1	0.742	0.742	0.6439

4. Conclusion

This work has tried to understand reactivity trends between Al_2O_3 and cryolite melts. When they are mixed, five- and six-fold motifs present in the cryolite melt might help to initiate the Al_2O_3 interaction by global hardness matching. When Al_2O_3 is within the vicinity, the main local interactions take place within the free fluorine regions of four-fold and five-fold clusters. Effects of implicit solvation on reactivity will be investigated as future work.

Acknowledgement

References

[1] C. M. Hall, "Process of reducing aluminium from its fluoride salts by electrolysis," US Patent No. 400,664 (1889).

[2] P. Héroult, French Patent No. 175,711 (1886).

[3] S. K. Padamata, A. S. Yasinskiy, P. V. Polyakov, "Electrolytes and its additives used in aluminum reduction cell," Metall. Res. Technol. 116 (2019) 410.

[4] Z. Akdeniz, Z. Çiçek, A. Karaman, G. Pastore, M. P. Tosi, "A Theoretical Study of the Stabilization of the $(AlF_5)^{2-}$ Complex Anion by Alkali Counterions," Z. Naturforsch 54 (1999) 575.

[5] R. R. Nazmutdinov, T. T. Zinkicheva, S. Y. Vassiliev, D. V. Glukhov, G. A. Tsirlina et al., "A spectroscopic and computational study of Al(III) complexes in sodium cryolite melts: Ionic composition in awide range of cryolite ratios," Spectrochimica Acta Part A 75 (2010) 1244.

[6] R. Li, L. Cheng, "Structural determination of $(Al_2O_3)_n$ ($n = 1$–7) clusters based on density functional calculation," Computational and Theoretical Chemistry 996 (2012) 125.

[7] R. R. Nazmutdinov, T. T. Zinkicheva, S. Y. Vassiliev, D. V. Glukhov, G. A. Tsirlina et al., "A spectroscopic and computational study of Al(III) complexes in cryolite melts: Effect of cation nature," Chemical Physics 412 (2013) 22.

[8] S. Cikit, Z. Akdeniz, P. A. Madden, "Structure and Raman Spectra in Cryolitic Melts: Simulations with an ab Initio Interaction Potential," J. Phys. Chem. B. 118 (2014) 1064.

[9] T. Bucko, F. Simko, "On the structure of crystalline and molten cryolite: Insights from the ab initio molecular dynamics in NpT ensemble," J. Chem. Phys. 144 (2016) 064502.

[10] K. Machado, D. Zanghi, V. Sarou-Kanian, S. Cadars, M. Burbano et al., "Study of $NaF-AlF_3$ Melts by Coupling Molecular Dynamics, Density Functional Theory, and NMR Measurements," J. Phys. Chem. C 121 (2017) 10289.

[11] T. Bucko, F. Simko,, "Effect of alkaline metal cations on the ionic structure of cryolite melts: Ab-initio NpT MD study," Metall. Res. Technol. 148 (2018) 064501.

[12] K. Machado, D. Zanghi, M. Salanne, V. Stabrowski, C Bessada, "Anionic Structure in Molten $Cryolite-Alumina$ Systems," J. Phys. Chem. C 122 (2018) 21807.

[13] M. Tan, T. Li, B. Shang, H. Cui, "Quantum chemical prediction of the spectroscopic properties and ionic composition of the molten $NaF-AlF_3$ salts," J. Mol. Liq. 317 (2020) 113937.

[14] R. G. Parr, W. Yang, "Density-Functional Theory of Atoms and Molecules," Oxford University Press, New York, (1989).

[15] P. Geerlings, F. De Proft, W. Langenaeker, "Conceptual Density Functional Theory," Chemical Reviews 103 (2003) 1793.

[16] P. K. Chattaraj, "Chemical Reactivity Theory; A Density Functional View," CRC Press, Boca Raton, (2009).

[17] A. S. Özen, Z. Akdeniz, "Structure and Bonding in Cryolitic Melts A Combined Study by Density Functional Theory and Ionic Model Calculations," Journal of Molecular Liquids Part B 368 (2022) 120771.

[18] R. G. Parr, R. A. Donnelly, M. Levy, W. E. Palke, "Electronegativity: The Density Functional Viewpoint," J. Chem. Phys. 68 (1978) 3801.

[19] R. G. Pearson, "Hard and soft acids and bases, HSAB, part 1: Fundamental principles," J. Chem. Educ. 45 (1968) 581.

[20] A. S. Özen, Z. Akdeniz, "Chemical Reactivity Perspective into the Group 2B Metals Halides," J. Phys. Chem. A 120 (2016) 4401.

[21] M. J. Frisch, G. W. Trucks, H. B. Schlegel, G. E. Scuseria, M. A. Robb, et al., "Gaussian 09, Revision C.01," Gaussian, Inc., Wallingford CT, (2016).

[22] X. Lv, Z. Xu, J. Li, J. Chen, Q. Liu, "Molecular dynamics investigation on structural and transport properties of $Na_3AlF_6 - Al_2O_3$ molten salts," Journal of Molecular Liquids 221 (2016) 26.

[23] Y. Zhang, X. Hu, M. Lin, A. Liu, Z. Shi, Z. Wang, "Quantum Chemical Calculation on the Decomposition Mechanism of Na_3AlF_6," Russian Journal of Physical Chemistry A 96 (2022) 1035.